

Dechanneling by dislocations: A model quantum-mechanical calculation

L. N. S. Prakash Goteti and Anand P. Pathak*

School of Physics, University of Hyderabad, Hyderabad 500 046, India

(Received 27 March 1998)

A quantum-mechanical treatment of the effects of dislocations on planar dechanneling is given. A simple harmonic model for planar potential due to two planes surrounding the channel and corresponding bound states in this transverse potential are considered. The transition probabilities among these states, due to distortions in the planar channel and the resulting dechanneling probabilities for varying distortion are calculated. The energy dependence of these dechanneling probabilities for initially well channeled particles has been estimated. [S0163-1829(98)07433-5]

I. INTRODUCTION

The effects of defects (both point defects as well as extended defects) on charged particle propagation along major crystallographic directions and planes have been studied for some time. The motivation has been to be able to use charged particle probes to study the materials for their purity because the properties like conductivity, stress, and tensile strength, etc., are influenced by the presence of defects. These defects have a great influence on the characteristic properties of the materials in general, and semiconductors in particular, where the formation of the dislocations during the growth modifies the properties like carrier density, lifetime of minority carrier, etc. Another motivation is to study the strain created vis-a-vis defects generated during growth of semiconductor devices like quantum well heterostructures.¹ In the case of point defects, one can study the related effects due to impurity scattering by evaluating, quantum mechanically, the corresponding scattering cross sections.² Similar quantum treatment for the effects of extended defects like dislocations has not been given so far.

The extended defects can be broadly classified between obstruction type (like stacking faults) and distortion type (like dislocations). Recently, we considered the dechanneling effects due to stacking faults, quantum mechanically.³ Here we present a quantum-mechanical model calculation for the dechanneling effects due to distortions of the planar channel caused by dislocations. The presence of dislocations and the resulting distortions affects the spectrum of channeled flux, even though the energy loss of well-channeled particles is not significantly affected.⁴ Classical calculations related to the effects of defects^{5,6} on channeling are good enough for heavier particles like protons, α particles, and heavy ions.⁷ However, the interaction of lighter particles like positrons and electrons with solids should be described quantum mechanically⁸ because these particles cannot be regarded as being localized but rather as an extended wave in the crystal.⁹ Moreover, these light particles are very sensitive to probe various kind of defects present in the solid.¹⁰ During the propagation of the channeled particles, the longitudinal energy is nearly constant and the motion is of a free particle type. In transverse space the particle sees a continuum potential due to an atomic string/plane. For positive particles like positrons, this may be approximated to a harmonic

oscillator-type potential for smaller amplitudes. With these basic concepts, a quantum-mechanical formulation is developed, and a description for dechanneling is given with specific reference to dislocations.

In this work we concentrate on a quantum-mechanical model for the effects of dislocations on initially well-channeled particles in a planar channel. For the case of stacking faults, the effect is obstruction type and the treatment is simple, whereas for the case of dislocations the channels are distorted and these distortion effects on channeling are incorporated by introducing an energy term $[(2E/R)x]$ due to transverse deflecting centrifugal force,¹¹ E being the average energy in the curved part of the channel with radius of curvature R and x being the position of the particle in a transverse direction. This term is to be added to the well-known continuum potential¹² surrounding the channel, which acts as a restoring force. We are considering the regions outside a critical region around the dislocations. The regions within that critical radius are distorted heavily, which leads to dechanneling of most of the particles arriving in that region. However, the regions outside that core region are only moderately affected, and the channeling and continuum model is still valid and used extensively by incorporating the effects of distortion through the above-mentioned centrifugal force term. The situation in these regions is similar to that found in the bending of beams by bent crystal channeling¹³ explained with continuum model. The condition is that bending should be less than the critical angle for channeling. The critical minimum radius of curvature R_{mc} of channels below which the particle will dechannel completely can be obtained by equating the deflecting centrifugal force to the restoring force due to planar potential, evaluated at the minimum distance of approach a_{TF} , and is given by^{11,14,15}

$$R_{mc} = \frac{4E}{\pi z_1 z_2 e^2 C N_p}$$

Here, $N_p = Nd_p = 2Nl$, with $d_p = 2l$ as width of the planar channel a_{TF} is the Thomas Fermi screening radius, C is the Lindhard constant given by $\sqrt{3}$, z_1 , z_2 are the atomic numbers of the projectile particle and target atom, respectively, and N is bulk density of atoms in the crystal.

All the particles coming in the channels with a radius of curvature less than R_{mc} will get dechanneled. Using the stan-

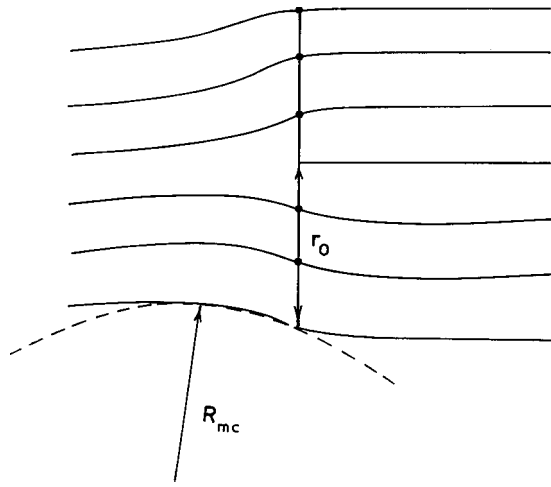


FIG. 1. The planar channels that are distorted due to presence of a dislocation. Here R_m is minimal radius of curvature of a typical channel situated at a distance r_0 .

dard displacement equations, the corresponding critical distance of such channels from the dislocation core r_0 is calculated.^{5,6,11} As shown in Fig. 1, the channels outside this region of radius r_0 around the dislocation core, called the dechanneling cylinder, are distorted slightly and result in only a slight modification of the state of motion of the channeled particles. We concentrate on the simplest case of screw dislocations with low concentrations so that there is no nucleation of dislocation loops. Here we consider the channels situated farthest from the dislocation axis. The amount of distortion present in a channel depends on the average concentration of the dislocations n . One can make an estimate for the farthest distance from the dislocation in terms of dislocation concentration [$r_0^{\max} = \frac{1}{2}(n^{1/2})$].

On the other hand, by solving the displacement equations for screw dislocation, the minimal radius of curvature is obtained from which one may obtain the mean dechanneling radius, and is given by⁵

$$r_0 = \sqrt{\left(\frac{bR_{mc}}{10}\right)}, \quad (1)$$

with b as the Burgers vector.

II. QUANTUM DESCRIPTION

We consider the motion of the positrons described in the rest frame of the particle. In this frame the particle ‘‘sees’’ the continuum potential $\gamma V(x)$ in the transverse direction because of the fact that for the relativistic energies, the continuum potential in the transverse space is enhanced by a factor of γ [$=1/\sqrt{(1-v_z^2/c^2)}$], due to the length contraction in the direction of propagation (z). When the particle enters into the distorted portion, the motion of the particle is modified due to the influence of the curvature, and in this distorted part of the channel the modified continuum potential as ‘‘seen’’ by the particle becomes $\gamma V_{\text{eff}}(x)$, which is written as

$$\gamma V_{\text{eff}} = \gamma V(x) - \gamma^2 m v_z^2 \left\{ \frac{b}{\pi} \frac{r_0(\gamma Z)}{(r_0^2 + \gamma^2 Z^2)^2} \right\} x. \quad (2)$$

The expression for the dechanneling radius r_0 in terms of the minimal critical radius of the curvature R_{mc} is obtained by equating the restoring force ($-\gamma dV/dy$) to the maximum value of the deflecting force due to curvature, as described in Sec. I and one may notice that, due to these relativistic effects, r_0 in Eq. (1) is enhanced by a factor of $\sqrt{\gamma}$.

As in the stacking fault case,³ the quantum description means transition among the energy levels in the transverse potential. These transitions are induced by the distortion created due to dislocations. As before, we use a harmonic oscillator model for the transverse potential and the sudden approximation for transitions. The coupling constant α (appearing in the normal harmonic oscillator model potential $\alpha = \sqrt{m_{\perp} \omega / \hbar}$) will change to α' in the distorted portion because the oscillation frequency of the particle gets modified in this distorted portion.

The force constant that is modified due to the distortion of the channel is obtained with the consideration of the harmonic approximation to the above effective planar potential. This analysis is appropriate for the channels that are situated far away from the dislocation, which in turn implies that we are considering crystals with low dislocation concentrations (typically, $10^6 - 10^8$ per cm^2).

Classically, initially a well-channeled particle in an undistorted region starts oscillating about the axis of the distorted channel. Once it enters into the distorted portion, the potential minimum is shifted due to curvature by an amount of, say a_r , which reduces the available space in the channel. The expression for the shift in the potential minimum a_r (about which the particle oscillates) in the distorted channel is obtained with an approximation, namely, neglecting fourth and higher-order terms of x/L that in turn means that we are dealing with those channels that are not heavily distorted (i.e., not very close to the dislocation axis). This in turn introduces a max. error of about 6% and the shift in the equilibrium axis is given by

$$a_r = \sqrt{\left(\frac{B^2}{L^2}\right) + \frac{L^2}{2}} - \frac{B}{L}; \quad B = \frac{RV_0 a_{\text{TF}}}{E}, \quad L = l + a_{\text{TF}}. \quad (3)$$

The channeling/dechanneling phenomena under this situation is governed by the overlap integrals of the appropriate wave functions in various regions. As shown in Fig. 2, there are three boundaries over which the particle has to cross during the passage through the distorted channel, to find itself again in a straight channel. These three boundaries are not so sharply well defined. However, for simplicity of the present (model) calculations, we use a sudden approximation to calculate the transition probabilities across these three boundaries, and, in what follows, we will identify these boundaries as three interfaces (I, II, and III). The wave function of the particle in different regions may be denoted as

$$\psi_i = \psi_L = \left(\frac{\alpha}{\sqrt{\pi} 2^i i!}\right)^{1/2} \exp\left\{-\frac{\alpha^2 x^2}{2}\right\} H_i(\alpha x), \quad (4)$$

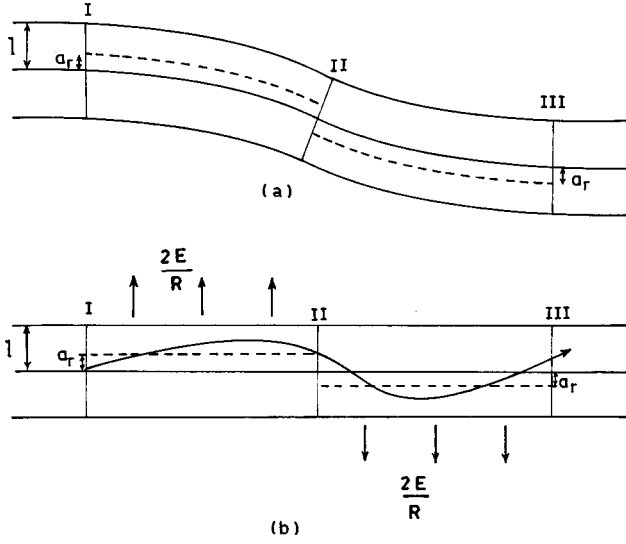


FIG. 2. (a) Typical planar channel of some finite curvature R . a_r is the shift in equilibrium position due to distortion. (b) Straight model channel replacing the channel of part (a). Here, I, II, and III are various portions of distortion through which the particle passes, and a_r is the equilibrium position about which the particle will oscillate.

$$\psi_j^{(1)} = \psi_I = \left(\frac{\alpha'}{\sqrt{\pi} 2^j j!} \right)^{1/2} \exp \left\{ \frac{-\alpha'^2 (x + a_r)^2}{2} \right\} \times H_j(\alpha' x + \alpha' a_r), \quad (5)$$

$$\psi_k^{(2)} = \psi_{II} = \left(\frac{\alpha'}{\sqrt{\pi} 2^k k!} \right)^{1/2} \exp \left\{ \frac{-\alpha'^2 (x - a_r)^2}{2} \right\} \times H_k(\alpha' x - \alpha' a_r), \quad (6)$$

$$\psi_f = \psi_R = \left(\frac{\alpha}{\sqrt{\pi} 2^f f!} \right)^{1/2} \exp \left\{ \frac{-\alpha^2 x^2}{2} \right\} H_f(\alpha x). \quad (7)$$

The maximum number of quantum states supported by a planar channel (surrounded by two planes) is estimated from the equation

$$(i_{\max} + \frac{1}{2}) \hbar \omega = \frac{1}{2} k x_{\max}^2. \quad (8)$$

with $\omega = \sqrt{k/\gamma m}$. To calculate the force constant, we consider the planar potential^{3,11-14}

$$V(x) = 2V_0 a_{TF} \left(\frac{1}{l + a_{TF} - x} + \frac{1}{l + a_{TF} + x} \right);$$

$$V_0 = \pi z_1 z_2 e^2 C a_{TF} N_p.$$

The maximum number of quantum states in undistorted continuum potential $i_{\max} = f_{\max}$ is found to be 3 for a specific case of 12.25 MeV ($\gamma = 25$) positrons channeled along Al(111). The number of quantum states available in the distorted portions 1 and 2 are estimated with the above procedure, replacing $V(x)$ by $V_{\text{eff}}(x)$ and found to be 1 ($j_{\max}^{(1)} = k_{\max}^{(2)} = 1$), corresponding to a channel situated at a distance of $15r_0$ from the dislocation [r_0 obtained from Eq. (1) and

for the present case of Al (111), b is taken as 2.86 \AA]. This $j_{\max}^{(1)}$ approaches i_{\max} for those channels, at the farthest distance from the core.

A. Channeling probabilities across (I) interface

The channeling probability of the particle with an initial state $|i\rangle$ to cross the first interface and to be in the state $|j\rangle$ in the distorted part can be defined as

$$p_{i \rightarrow j} = |\langle \psi_j^{(1)} | \psi_i \rangle|^2, \quad (9)$$

where the subscript 1 in the state denotes the relevant wave function that corresponds to the distorted channel after the I interface. The corresponding probability of occupying any one of the states $|j\rangle$ ($j_{\max} < i_{\max}$) is

$$p_i^1 = \sum_{j=0}^{j_{\max}} |\langle j^{(1)} | i \rangle|^2. \quad (10)$$

So the dechanneling probability at (I) is $\chi_i^1 = 1 - p_i^1$. We introduce a parameter τ such that $\alpha' = \tau\alpha$, which represents distortion effects. The evaluation of the above integrals is straightforward, though laborious, and the details are given in the Appendix.

B. Channeling probabilities across the (II) interface

The channeling probability of the particle with the intermediate state $|j\rangle$ to cross the second interface and to occupy a state $|k\rangle$ can be defined as

$$p_{j \rightarrow k} = |\langle \psi_k^{(2)} | \psi_j^{(1)} \rangle|^2. \quad (11)$$

Here the subscript 2 denotes the wave function in the second part of the distorted channel after crossing the II interface.

Corresponding the probability of the particle to occupy any one of the states $|k\rangle$ ($k_{\max} < i_{\max}$) is

$$p_{j(1)}^{\text{II}} = \sum_{k=0}^{k_{\max}} |\langle k^{(2)} | j^{(1)} \rangle|^2; \quad \chi_{j(1)}^{\text{II}} = 1 - p_{j(1)}^{\text{II}}. \quad (12)$$

To evaluate the various matrix elements in this case, we make use of the general expression obtained for $\langle j | k \rangle$ in our recent work,³ and one may easily verify that $|\langle k^{(2)} | j^{(1)} \rangle|^2 = |\langle j^{(2)} | k^{(1)} \rangle|^2$.

C. Channeling probabilities across the (III) interface

The channeling probability of the particle with intermediate state $|k\rangle$ to cross the third interface and to occupy any one of the states $|f\rangle$ ($f \leq i$) is

$$p_k^{\text{III}} = \sum_{f=0}^3 |\langle f | k^{(2)} \rangle|^2; \quad \chi_k^{\text{III}} = 1 - p_k^{\text{III}}, \quad (13)$$

with

$$p_{k(3) \rightarrow f} = |\langle f | k^{(2)} \rangle|^2. \quad (14)$$

For example,

$$p_{0(2) \rightarrow 0}^{(3)} = |\langle 0 | 0^{(2)} \rangle|^2 = 2\beta E x = |\langle 0^{(1)} | 0 \rangle|^2.$$

Similarly, one can obtain other amplitudes and verify that $|\langle f|k^{(2)}\rangle|^2 = |\langle j^{(1)}|i\rangle|^2$ for the same quantum numbers of k and j . The transition probability for the passage of an initially well-channeled particle through dislocation will be the product of the transition probabilities across various parts of the channel where the effects of distortion are suitably incorporated. The general expression for the total channeling probability of the particle with a specific initial state $|i\rangle$ so that the particle feels itself again in the straight channel with final state $|f\rangle$ (after passing through the various portions of distortion) has been obtained and is given by

$$p_{i \rightarrow f} = \sum_{k^{(2)}=0}^{k_{\max}^{(2)}} \left(p_{k^{(2)} \rightarrow f} \left[\sum_{j^{(1)}=0}^{j_{\max}^{(1)}} p_{i \rightarrow j^{(1)}} \times p_{j^{(1)} \rightarrow k^{(2)}} \right] \right) = p_{f \rightarrow i}. \quad (15)$$

The total channeling probability for an initially well-channeled particle to find itself again in the straight channel after passing through various portions of the distortions is given by

$$p_0 = \sum_{f=0}^{f_{\max}=3} (p_{0 \rightarrow f}); \quad \chi_0 = 1 - p_0. \quad (16)$$

III. RESULTS AND CONCLUSIONS

We have developed a quantum theory of dechanneling due to defects with special reference to dislocations. The theory is valid as long as the number of quantum states supported by the transverse potential due to the two planes is small. This happens for light particles like positrons in the MeV range. We studied the dechanneling processes by continuous distortions of the planar channels, mapping to three distinct regions (Fig. 2) and corresponding displaced and modified wave functions. This happens for channels far away from the dislocation, which in turn implies applicability of the present calculation to lower concentrations (i.e., no interaction between dislocations). On the other hand, for channels close to the dislocation axis, the distortion is so heavy that one cannot talk of crystallographic channels (see Fig. 1).

In Fig. 3(a), we have shown a variation of a max. number of allowed states in the distorted channel as a function of distance from the dislocation. The atomic planes at considerably larger distances from the core are distorted slightly and thus r_0 carries the signature of the distortion effects. We notice that j_{\max} approaches asymptotically to $i_{\max}(=3)$ as r_0 increases (i.e., the channel is almost straight). As mentioned earlier, this depends on the concentration of dislocations. Thus, for lower concentrations, we have a family of channels through which a particle can propagate successfully without much dechanneling. We consider the channels starting from $15r_0$ (this corresponds to a concentration $\approx 3 \times 10^8$ dislocations/cm², below this the channels are distorted heavily leading to the formation of dislocation loops) to a farthest distance $50r_0$ (this dislocation concentration is typically $\approx 2 \times 10^7$ /cm²). In Fig. 3(b), we show the variation of the distortion parameter τ with r_0 . We notice that, for larger r_0 , the radius of curvature (R) of the distorted planar channel increases to infinity, $a_r \rightarrow 0$ and $\tau \rightarrow 1$ as expected, because the coupling terms in the wave functions are identical,

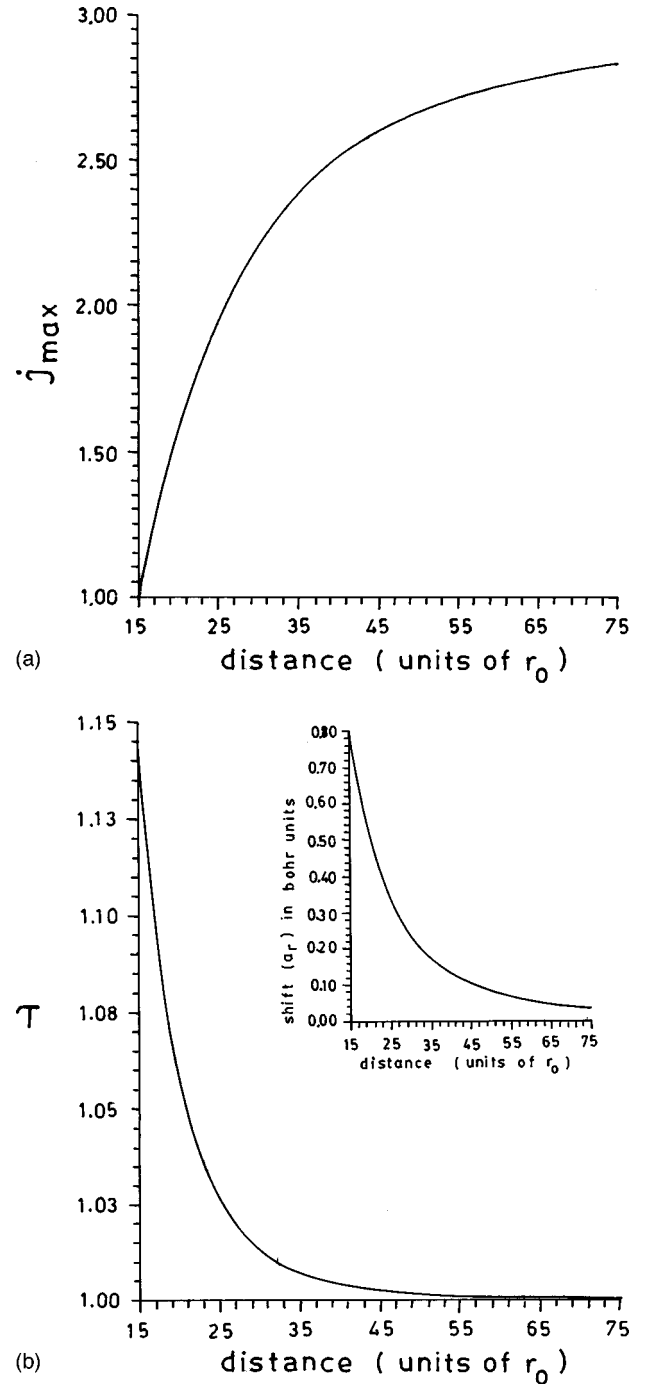
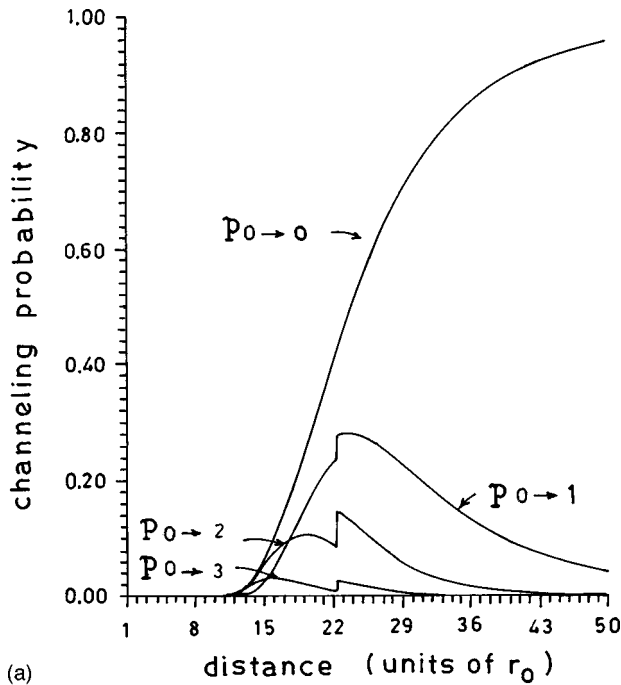


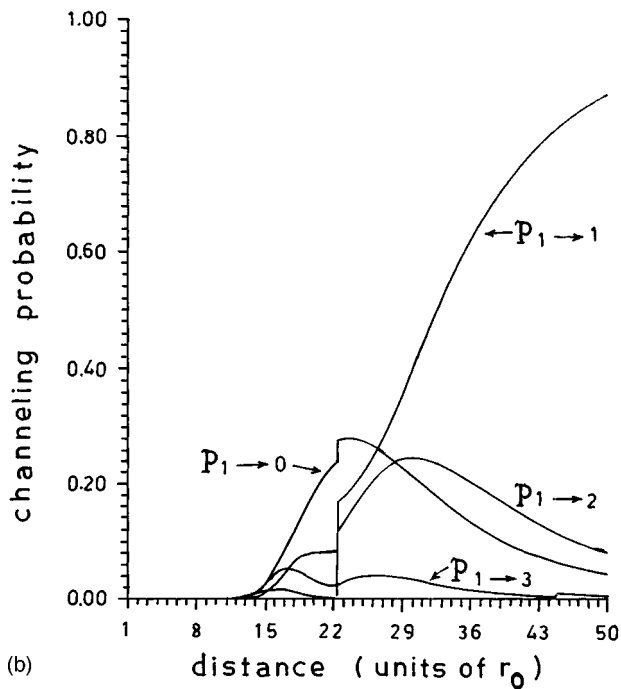
FIG. 3. (a) The variation of number of states supported by a planar channel with distortion of the channel where these effects are expressed in units of r_0 . (b) The variation of distortion parameter τ ($\tau = \alpha'/\alpha$) as a function of distance from the dislocation.

the particle recognizes the absence of distortions in those regions and obviously the nondiagonal matrix elements vanish for $a_r = 0$, implying that a well-channeled particle cannot suddenly go to oscillatory behavior in an undistorted channel.

The results for channeling probabilities obtained from expressions (15) and (16) have been plotted in Figs. 4 and 5 for an initially well-channeled particle (i.e., ground state) and first excited state, respectively. One may notice that, at some values of r_0 , there is a sharp increase in the probability for individual transitions. This is a result of the change in the



(a)



(b)

FIG. 4. (a) Influence of channel distance from the dislocation on channeling probabilities corresponding to an initially well-channeled particle ($|i\rangle=|0\rangle$). (b) Influence of the channel distance from the dislocation on channeling probabilities corresponding to the initial state $|1\rangle$.

number of states supported in the distorted portions of the channel (i.e., after the I and II interfaces). This is also reflected in the overall dechanneling probabilities χ_0 and χ_1 , respectively, because corresponding channeling probabilities approach unity for the channels situated farthest from the dislocation axis, which means that a slight dissociation of dislocations reduces their long-range distortion, as discussed in classical analysis.⁶ As expected, the overall dechanneling probabilities for an initially well-channeled particle (χ_0) is

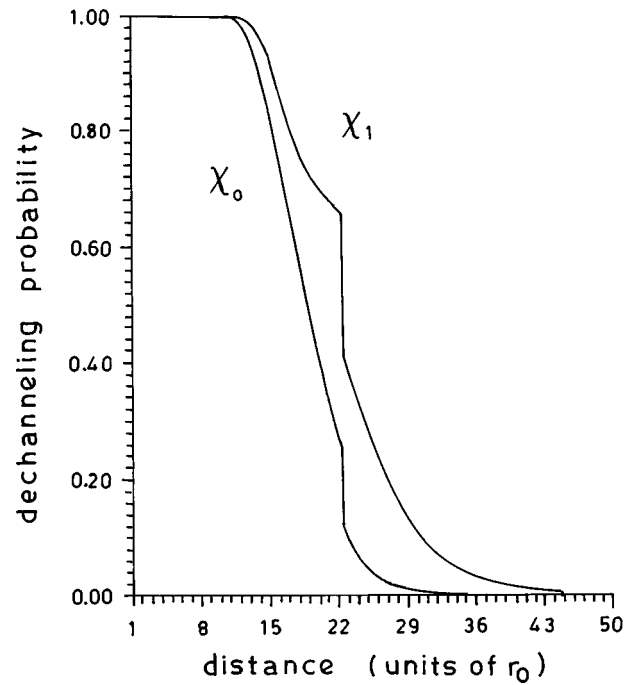


FIG. 5. Influence of the channel distance from the dislocation on total dechanneling probabilities for the initial state $|0\rangle$ and $|1\rangle$ denoted by χ_0 and χ_1 , respectively.

always less for any channel as compared to χ_1 (particle initially in the first excited state) because a well-channeled particle, even after making transitions to other excited states in distorted portions of the channel, manages to remain channeled for higher curvatures (lesser radii of curvatures) than does the initially excited (oscillating) particle. In the present simple model calculation, these effects are manifested in a natural way.

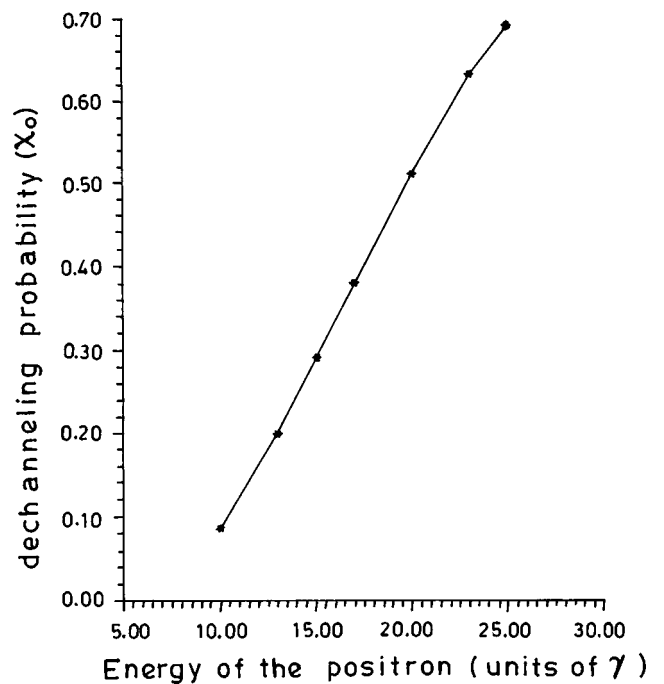


FIG. 6. Energy dependence of total dechanneling probability of the initially well-channeled particle χ_0 .

If the particle, after passing through various portions of distortions, goes to a state which is the same as the initial state, the corresponding channeling/transition probability is much higher as compared to other transitions. This is expected, and can also be seen through the asymmetric nature of the planar channel. The channeling probabilities, corresponding to a different initial and final-state combination, are very low, and approach zero as the channel distance increases from the dislocation. So, the dechanneling probability depends upon the final state of the particle, which in turn reflects the phase dependence of the approaching particle near the distortion.

Equation (15) carries the signature of an interesting left-right symmetry built into the problem that is not clearly re-

alized in classical descriptions. Figure 6 shows the energy dependence of dechanneling probabilities for initially well-channeled particles. At the lower end of these relativistic energies, it is linear in variation, and as the energy increases to the higher side of the relativistic energy, the energy dependence tends to be slower than linear.

ACKNOWLEDGMENTS

L.N.S.P.G. is grateful to the University Grants Commission for financial support. A.P.P. thanks Professor Yu Lu and Professor P. N. Butcher for hospitality at ICTP, Trieste, Italy.

APPENDIX: EVALUATION OF INDIVIDUAL TRANSITION AMPLITUDES: $|\langle j^{(1)}|i\rangle|^2$

We have

$$|\langle j^{(1)}|i\rangle|^2 = \left(\frac{\alpha\alpha'}{\pi 2^{j^{(1)}+i} j^{(1)}! i!} \right) \exp\left\{ - \left(\frac{\alpha'^2}{\alpha^2 + \alpha'^2} \right) \alpha^2 a_r^2 \right\} \\ \times \left| \int_{-\infty}^{\infty} \exp\left\{ - \frac{1}{2} (\alpha^2 + \alpha'^2) \left[x + \frac{\alpha'^2}{\alpha^2 + \alpha'^2} a_r \right] \right\} H_j(\alpha'x + \alpha'a_r) H_i(\alpha x) \right|^2.$$

Here we denote $\beta = \tau/(1 + \tau^2)$; $\xi = \tau^2/(1 + \tau^2)$, and $Ex = \exp\{-\xi\alpha^2 a_r^2\}$, and this notion makes the final expressions for transition amplitudes more compact. By substituting the Hermitian functions corresponding to various states and evaluating the integrals, the expressions for individual transition amplitudes are obtained, and they are

$$|\langle 0^{(1)}|0\rangle|^2 = 2\beta Ex,$$

$$|\langle 1^{(1)}|0\rangle|^2 = 4\beta^3 \alpha^2 a_r^2 Ex,$$

$$|\langle 2^{(1)}|0\rangle|^2 = \frac{\beta}{4} \left[4\beta^2 \alpha^2 a_r^2 - 2 \left(\frac{1 - \tau^2}{1 + \tau^2} \right) \right]^2 Ex,$$

$$|\langle 3^{(1)}|0\rangle|^2 = \frac{\beta}{24} [\alpha a_r (24\tau\xi^2 - 36\tau\xi + 12\tau) + \alpha^3 a_r^3 (8\tau^3 \xi^3 + 24\tau\xi^2 - 8\tau^3)]^2 Ex,$$

$$|\langle 0^{(1)}|1\rangle|^2 = 4\beta\xi^2 \alpha^2 a_r^2 Ex$$

$$|\langle 1^{(1)}|1\rangle|^2 = 8\beta^3 [1 - \xi\alpha^2 a_r^2]^2 Ex,$$

$$|\langle 2^{(1)}|1\rangle|^2 = \frac{\beta}{8} [\alpha a_r (24\xi^2 - 20\xi) + \alpha^3 a_r^3 (8\tau^2 \xi^3 - 16\tau^2 \xi^2 + 8\tau^2 \xi)]^2 Ex,$$

$$|\langle 3^{(1)}|1\rangle|^2 = \frac{\beta}{48} [(48\beta\xi - 24\beta) + \alpha^2 a_r^2 (96\tau\xi^3 - 168\tau\xi^2 + 72\tau\xi) + \alpha^4 a_r^4 (16\tau^3 \xi^4 + 48\tau\xi^3 - 16\tau^3 \xi)]^2 Ex,$$

$$|\langle 0^{(1)}|2\rangle|^2 = \frac{\beta}{4} \left[2 \left(\frac{1 - \tau^2}{1 + \tau^2} \right) + 4\xi^2 \alpha^2 a_r^2 \right]^2 Ex,$$

$$|\langle 1^{(1)}|2\rangle|^2 = \frac{\beta}{8} [8\beta\xi^2 \alpha^3 a_r^3 + 4\beta\alpha a_r - 24\beta\xi\alpha a_r]^2 Ex,$$

$$|\langle 2^{(1)}|2\rangle|^2 = \frac{\beta}{32} [48\beta^2 + \alpha^2 a_r^2 (96\tau^2 \xi^3 - 96\xi^2 + 8\tau^2 \xi + 16\xi - 8\tau^2) + \alpha^4 a_r^4 (16\tau^2 \xi^4 - 32\tau^2 \xi^3 + 16\tau^2 \xi^2) - 4]^2 Ex,$$

$$|\langle 3^{(1)}|2\rangle|^2 = \frac{\beta}{192} [\alpha a_r (-480\beta\xi^2 + 432\beta\xi + 48\tau\xi^2 - 48\beta - 72\tau\xi + 24\tau)$$

$$+ \alpha^3 a_r^3 (-320\tau\xi^4 + 624\tau\xi^3 - 336\tau\xi^2 + 16\tau^3\xi^3 + 32\tau\xi + 48\tau\xi^3 - 16\tau^3) + \alpha^5 a_r^5 (-32\tau^3\xi^5 - 96\tau\xi^4 + 32\tau^3\xi^2)]^2 Ex,$$

$$|\langle 0^{(1)}|3\rangle|^2 = \frac{\beta}{24} [12\xi\alpha a_r - 24\beta^2\alpha a_r - 8\xi^3\alpha^3 a_r^3]^2 Ex,$$

$$|\langle 1^{(1)}|3\rangle|^2 = \frac{\beta}{48} \left[24 \left(\frac{1-\tau^2}{1+\tau^2} \right) \beta + 96\beta\xi^2\alpha^2 a_r^2 - 48\beta\xi\alpha^2 a_r^2 - 16\beta\xi^3\alpha^4 a_r^4 + 24\beta\xi\alpha^2 a_r^2 \right]^2 Ex,$$

$$|\langle 2^{(1)}|3\rangle|^2 = \frac{\beta}{192} [\alpha a_r (144\xi^2 - 480\beta^2\xi - 120\xi + 240\beta^2) + \alpha^3 a_r^3 (-320\xi^4 + 48\tau^2\xi^3 + 400\xi^3 - 96\xi^2 - 96\tau^2\xi^2 + 48\tau^2\xi) + \alpha^5 a_r^5 (-32\tau^2\xi^5 - 32\tau^2\xi^3 + 64\tau^2\xi^4)]^2 Ex,$$

$$|\langle 3^{(1)}|3\rangle|^2 = \frac{\beta}{1152} \left\{ \left[960\beta^3 - 288\beta\xi - 144\beta \left(\frac{1-\tau^2}{1+\tau^2} \right) \right] + \alpha^2 a_r^2 (2880\beta\xi^3 - 3456\beta\xi^2 + 1008\tau\xi^2 + 864\beta\xi - 576\tau\xi^3 - 432\tau\xi) + \alpha^4 a_r^4 (960\tau\xi^5 - 2016\tau\xi^4 - 96\tau^3\xi^4 + 288\tau^3\xi^3 + 1248\tau\xi^3 - 192\tau\xi^2 - 288\tau^3\xi^2 + 96\tau^3\xi) + \alpha^6 a_r^6 (64\tau^3\xi^6 - 192\tau^3\xi^5 + 192\tau^3\xi^4 - 64\tau^3\xi^3) \right\}^2 Ex.$$

*Author to whom correspondence should be addressed. Present address: Fakultat für Physik, Universität Freiburg, Herman Herder Str. 3 79104 Freiburg, Germany. Fax: +49 761 203 5883; electronic address: pathak@phyc1.physik.uni-freiburg.de

¹A. Kozanecki, J. Kaczanowski, B. J. Sealy, and W. P. Gillin, Nucl. Instrum. Methods Phys. Res. B **118**, 640 (1996); for a review, see, for example, J. W. Mayer, Radiat. Eff. **12**, 183 (1972).

²Azher M. Siddiqui, V. Harikumar, L. N. S. Prakash Goteti, and Anand P. Pathak, Mod. Phys. Lett. B **10**, 745 (1996).

³L. N. S. Prakash Goteti and Anand P. Pathak, J. Phys.: Condens. Matter **9**, 1709 (1997).

⁴P. K. Bhattacharya, J. Chevallier, E. Uggerhøj, J. More, and Y. Quere, Radiat. Eff. **51**, 127 (1980); A. P. Pathak, Phys. Lett. **55A**, 104 (1975); **57A**, 467 (1976).

⁵Y. Quere, Phys. Status Solidi **30**, 713 (1968).

⁶J. Mory and Y. Quere, Radiat. Eff. **13**, 57 (1972).

⁷S. T. Picraux, E. Rimini, G. Foti, and S. Campisano, Phys. Rev. B **18**, 2078 (1978).

⁸F. Grasso, M. Lo Savio, and E. Rimini, Radiat. Eff. **12**, 149 (1972); M. A. Kumakhov and R. Wedell, Phys. Status Solidi B

84, 581 (1977).

⁹R. E. DeWames, W. F. Hall, and G. W. Lehman, Phys. Rev. **148**, 181 (1966); **174**, 392 (1968); A. P. Pathak, Phys. Rev. B **7**, 4813 (1973).

¹⁰Peter. J. Schultz, Guiti R. Massoumi, and W. N. Lennard, Nucl. Instrum. Methods Phys. Res. B **90**, 567 (1994).

¹¹A. P. Pathak, Phys. Rev. B **13**, 4688 (1976).

¹²A. P. Pathak, Radiat. Eff. **61**, 1 (1982); A. P. Pathak and S. Satpathy, Nucl. Instrum. Methods Phys. Res. B **33**, 39 (1988); A. P. Pathak and B. Rath, Radiat. Eff. **63**, 227 (1982).

¹³Richard A. Carrigan, Jr., Timothy E. Toohing, and Edica N. Tsyganov, Nucl. Instrum. Methods Phys. Res. B **48**, 167 (1990); M. A. Khumakov, *ibid.* **48**, 167 (1990); W. M. Gibson, I. J. Kim, M. Pisharody, S. M. Salman, C. R. Sun, G. H. Wang, R. Wijayawardana, J. S. Forster, I. V. Mitchell, T. S. Nigmanov, E. N. Tsyganov, S. I. Baker, R. A. Carrigan, Jr., T. E. Toohig, V. V. Avdeichikov, J. A. Ellison, and P. Siffert, *ibid.* **2**, 54 (1984).

¹⁴Anand P. Pathak, Radiat. Eff. **30**, 193 (1976).

¹⁵Hiroshi Kudo, Phys. Rev. B **18**, 5995 (1978); Konrad Gartner and Arnaldo Uguzzoni, Nucl. Instrum. Methods Phys. Res. B **67**, 189 (1992).